

Doublet structure of nonspecular x-ray scattering from multilayers

B. Lai, W. B. Yun, J. Chrzas, and P. J. Viccaro

Advanced Photon Source, Argonne National Laboratory, 9700 South Cass Avenue, Argonne, Illinois 60439

(Received 19 February 1992)

The nonspecular scattering of x rays from a multilayer structure deposited on Pt film was studied experimentally. The study resolved the long-standing problem of the origin of the doublet structure first observed about three decades ago. A model based on coherent interfering fields, with the traveling component of the interference field propagating parallel to the interface, is proposed to explain the effect. The implication of the existence of the doublet structure for both specular and nonspecular x-ray-interference measurements is discussed.

INTRODUCTION

Various x-ray-interference techniques have been employed for thin-film structural studies since the pioneering work by Kiessig.¹ In Kiessig's original work, the thickness of a film was determined by the interference modulation to the specular reflectivity measured over a range of incident angles. This specular reflectivity technique has been employed for the study of a broad range of material systems and phenomena, such as *in situ* studies of electrode surfaces,² microemulsion surfaces,³ and organic monolayers.⁴ On the other hand, interference of nonspecularly reflected x rays was used by Sauro to measure thin film thickness.⁵ This group concluded that the utilization of their technique may be more favorable than that of specular reflection for precise determination of film thickness. This technique was subsequently used by Kapp and Wainfan to study stearate multilayer films.⁶ In the later work, principal maxima in the interference fringes were observed, which can be attributed to asymmetric Bragg scattering by the multilayer periodicity. In particular, they observed a set of interference fringes that they called a doublet structure. The doublet structure occurs only for small angle of incidence, and the origin of the doublet structure remained unexplained. In this work, we report experimental and theoretical evidence of the origin of the doublet structure. The implication of the existence of the doublet structure for both specular and nonspecular x-ray-interference measurement is discussed.

EXPERIMENT

The experimental setup is shown schematically in Fig. 1(a). X rays from a sealed Cu tube (2-kW power) were monochromated by reflecting from a Si(111) crystal and were collimated with two slits each of 0.1-mm width placed before and after the crystal, reducing the angular divergence to 0.32 mrad. Cu $K\alpha_1$ radiation ($\lambda = 1.541 \text{ \AA}$) of 0.12% bandwidth ($\Delta\lambda/\lambda$) was directed toward the sample at a glancing incident angle. The sample was mounted on the θ rotation stage of a precision θ - 2θ diffractometer. On the 2θ rotation arm, a NaI scintillation counter and a narrow slit were located at 49.8 cm

from the center of rotation to collect radiation scattered from the sample. The slit with a width of 0.3 mm provided an angular definition of about 0.035° .

The sample consisted of a 250- \AA Pt film sputtered onto a flat Si(001) substrate, and a Si/W multilayer deposited over the Pt. Because the x-ray refractive indices of Pt and the multilayer are less than unity, there exists a critical angle for total reflection for each of the materials. For Pt, the critical angle is $\alpha_c^{\text{Pt}} = 0.57^\circ$ at the Cu $K\alpha$ radiation. Below the critical angle, the e -fold penetration depth for x rays in Pt is $\approx 10 \text{ \AA}$, and it increases to 54 \AA at the critical angle.⁷ The 250- \AA Pt film is thus thick enough to reflect all incoming x rays for glancing angles of incidence less than α_c^{Pt} . Above the Pt is a Si/W multilayer, which has been shown to be an efficient reflector in the hard x-ray region.⁸ For our experiment, a 10-period multilayer with d spacing of 46.6 \AA was deposited over the Pt film. To reduce absorption, the W-layer thickness was made to be $\frac{1}{4}$ that of the Si layer. The low W-to-Si ratio also serves to limit the average multilayer critical angle (α_c^{ml}) to be less than the Pt criti-

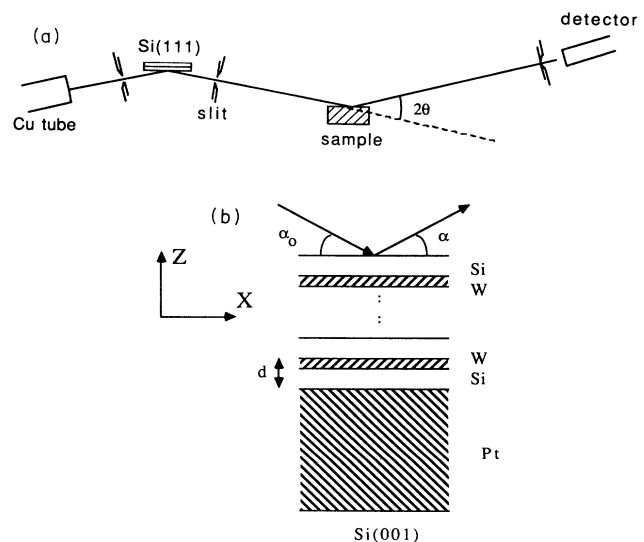


FIG. 1. Schematic of (a) the experimental setup, (b) the sample, and the notation used in the text.

cal angle. Thus, there exists a range of incident angles, $\alpha_c^{ml} < \alpha_0 < \alpha_c^{Pt}$, in which the x rays can penetrate into the multilayer and be totally reflected by the Pt film. A null sample was also fabricated that consisted of an identical Si/W multilayer deposited on the same substrate but without the Pt film. For the null sample, α_c^{ml} is larger than the critical angle of the material beneath it (namely, Si). Both samples were prepared under identical conditions in an 8-in.-targets rf-sputtering system.

Figure 2 shows the specular reflectivity measured by conventional θ - 2θ scans on the two samples. The critical angle of the Si/W multilayer is seen at 0.32° for both curves (α_c^{ml}), while the one at 0.57° for the solid line is due to the Pt film (α_c^{Pt}). In the region between these two critical angles, intensity modulations are observed in the reflectivity spectra that continue into higher angles. The modulations are produced by interference of x rays reflected from the two interfaces, at the first and the last layers, of the multilayer.^{1,6} The existence of modulations indicates that the two interfaces have adequate flatness. The quality of the multilayer is also evident from the high reflectivity measured on the first-order Bragg peak at $\alpha_0 = 1^\circ$. For the null sample, the Bragg peak appears at about the same angle (similar d spacing), and there is no critical angle due to Pt.

To study the nonspecular scattering, angular intensity of the scattered x rays was measured by scanning the detector in the 2θ ($=\alpha + \alpha_0$) direction while the incident angle α_0 was held fixed. The results for incident angles less than and slightly above α_c^{Pt} are shown in Fig. 3. In all the spectra, a peak was found at about 2° . This peak is caused by the multilayer imparting a momentum of $2\pi/d$ to the incident beam in the z direction

$$\Delta k_z = 2\pi/d \rightarrow \sin\alpha + \sin\alpha_0 = \lambda/d. \quad (1)$$

For small angles, the angle of deflection $\alpha + \alpha_0$ is a constant $\lambda/d = 2.02^\circ$, where λ is the x-ray wavelength in the multilayer. Equation (1) is equivalent to the usual Bragg condition for predicting diffraction maximum, except that the scattering angle α is not required to be identical to the incidence angle α_0 . This peak was observed on both samples because it is caused by momentum transfer from the multilayer. At very glancing incident angles,

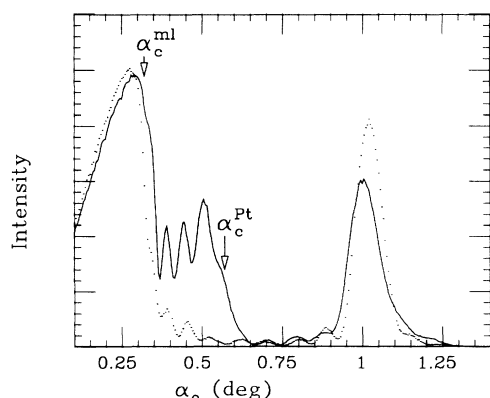


FIG. 2. Specular reflectivity (θ - 2θ) spectra on sample with (solid line) and without (dotted line) the Pt layer.

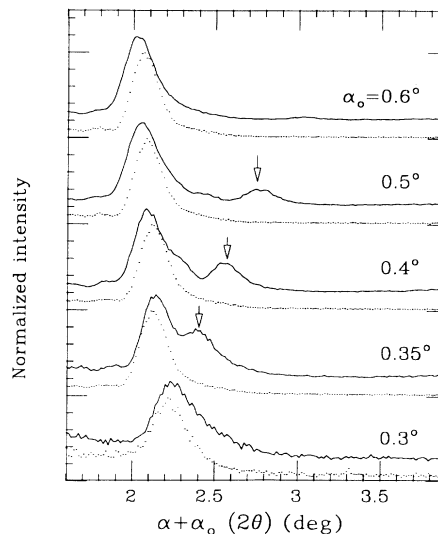


FIG. 3. Scattered intensity as a function of the deflection angle. Solid lines: sample with Pt layer. Dots: null sample. The intensities have been normalized.

the peak gradually shifted toward higher angles simply due to increased refraction.⁹ These nonspecular scatterings can, in turn, be used for accurate measurements of the d spacing, and have been utilized for that purpose.⁶

A second anomalous peak (indicated by arrows in Fig. 3) was also observed on the sample with the Pt film. This peak was discernible within a limited range of the incident angles, namely, $\alpha_c^{ml} < \alpha_0 < \alpha_c^{Pt}$. The fact that it largely disappeared when the incident angle was greater than α_c^{Pt} indicates it relied on the high reflectivity of the Pt. At the other limit, when the incident angle became less than α_c^{ml} , x rays could not penetrate through the multilayer and no interference was present. In between the two critical angles, the peak moved to smaller angles as α_0 decreased. Previously, a similar doublet structure in the scattering was recorded using photographic film for a Langmuir-Blodgett multilayer deposited on a glass surface, but its origin was not known.⁶ In that case, the glass substrate also had a critical angle larger than that of the barium stearate film.

THEORY AND DISCUSSION

This anomalous peak can be explained by considering diffraction of a traveling wave by the multilayer structure. The traveling wave is a dynamic component of the interference field set up between the incident beam and the beam reflected from the Pt surface. Using the reference system of Fig. 1(b), the total interference wave field $A(x, z, \mathbf{k}, \mathbf{k}')$ is given by

$$\begin{aligned} A(x, z, \mathbf{k}, \mathbf{k}') &= e^{i(\mathbf{k} \cdot \mathbf{R} - \omega t)} + r e^{i(\mathbf{k}' \cdot \mathbf{R} - \omega t)} \\ &= 2|r| \cos(k_z z + \phi/2) e^{i(k_x x - \omega t + \phi/2)} \\ &\quad + (1 - |r|) e^{i(k_x x - k_z z - \omega t)}, \end{aligned} \quad (2)$$

where r ($=|r|e^{i\phi}$) is the Fresnel reflection coefficient, \mathbf{k} and \mathbf{k}' are the wave vectors of the incident and the

reflected beam, respectively, and ω is the angular frequency of the electric field. The phase shift ϕ is determined by the incident angle and the refractive indices of the two media involved. The value of ϕ varies from π to 0 as the glancing incident angle increases from 0° to the critical angle α_c .¹⁰ The first term of Eq. (2) represents a traveling wave propagating parallel to the surface. The amplitude of this traveling wave, $2|r|\cos(k_z z + \phi/2)$, is a sinusoidal function of the z coordinate normal to the surface. The second term of Eq. (2) represents a wave propagating in the direction of the incident wave with an amplitude of $1 - |r|$, which is much less than unity when the x rays are totally reflected. The intensity distribution of the interference field is given by the absolute square of $A(x, z, \mathbf{k}, \mathbf{k}')$, which yields the well-known static standing-wave field normal to the surface in the total reflection regime.¹⁰ The nodes and antinodes of the standing wave will occupy various z locations for different incident angles, as r is a function of α_0 . Techniques based on the standing-wave properties have been successfully applied to probe the interfacial structures and elemental distribution of many material systems.¹¹

The traveling component of the interference field established by total reflection has not been previously investigated in detail. In the presence of the multilayer, the wave front of the traveling component is modified to

$$I(\alpha) \sim \left| \sum_m \int e^{ik_x x} T(x) \int [e^{ik_z z} + r e^{-ik_z z}] t_m e^{i(2\pi m/d)z} e^{i(k \sin \alpha)z} dz dx \right|^2. \quad (4)$$

The total phase factor inside the z integral is thus stationary in z only when

$$\sin \alpha = m \lambda / d \pm k_z / k = m \lambda / d \pm \sin \alpha_0. \quad (5)$$

Therefore, for each of the m th-order expansion terms of $T(x, z)$, there are two diffraction peaks with an angular splitting of $2 \sin \alpha_0$. For small angles, the splitting decreases linearly with the incident angle, which is in agreement with our experimental data in Fig. 3. If the standing-wave period ($\lambda / \sin \alpha_0$) is smaller than the d spacing, the splitting will be large enough that peaks from different orders will overlap. For our sample, the period of the standing wave is 155 \AA at α_c^{Pt} , and therefore no overlap of orders will occur. Note for the null sample $r \approx 0$, and the condition for angular maxima reduces to Eq. 1.

The diffraction intensity calculated based on Eq. (3) for a 10-period multilayer is shown in Fig. 4, after correcting α and α_0 for refraction at the air-multilayer interface. In the calculation, we assumed for simplicity that the x-ray transmission is $T(x, z) = 1$ for Si layers, and $T(x, z) = 0$ for W layers. At the first order ($m = 1$), there is splitting in the diffraction peak (A and B) as predicted, and the calculated peak positions agree very well with the experimental results. The difference in the intensities of A and B is caused by the nonsymmetric amplitude distribution of the interference field $A(x, z)$, due to nonideal reflection from Pt ($|r| < 1$) and absorptions of the incident and

different extents by the alternating material layers. The situation is similar to a diffraction grating with open and opaque zones that disturb the wave front of an illumination wave (the traveling wave in our case). The traveling wave will be diffracted, and the diffraction intensity will depend on the strength of the interference field and the difference in the refractive indices between individual layers. The Si-W system is a good materials combination for obtaining high diffraction intensity. In W the length for the π -phase shift of the x ray relative to vacuum is $1.7 \mu\text{m}$, and is $10 \mu\text{m}$ in Si. The absorption length is $3.1 \mu\text{m}$ in W for Cu $K\alpha$ x rays, versus $70 \mu\text{m}$ in Si. The tungsten layers thus introduce a larger phase delay and stronger intensity attenuation to the traveling wave compared to the adjacent Si layers. Assuming unit amplitude for the incident beam, the diffracted intensity $I(\alpha)$ may be calculated using the Fraunhofer integral¹²

$$I(\alpha) \sim \left| \int \int A(x, z) T(x, z) e^{ikz \sin \alpha} dz dx \right|^2, \quad (3)$$

where $A(x, z)$ is the interference field defined in Eq. (2), and $T(x, z)$ is the transmission function of the multilayer.

Because $T(x, z)$ is periodic in z with period d , it can be expanded in a Fourier series of the form $\sum_m t_m e^{i(2\pi m/d)z}$, where m represents integers. Using $T(x)$ to denote the x dependence of $T(x, z)$, the diffraction intensity becomes

reflected beam in the multilayer. In other words, when the actual optical constants of Si, W, and Pt were used for the calculation, the wave vector \mathbf{k} has both real and imaginary parts, and the reflected beam has an amplitude smaller than unity. Overall, the calculated results agree very well with the measured data. For three different in-

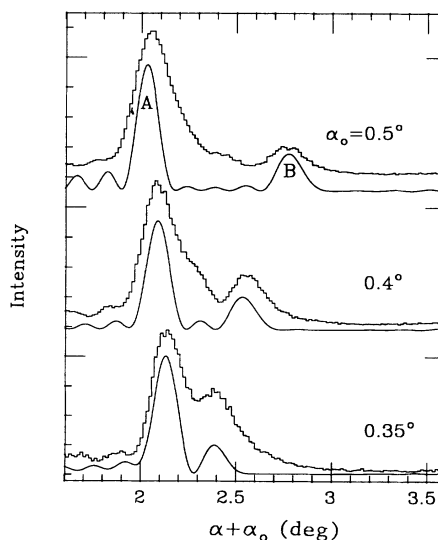


FIG. 4. Histogram: experimental data. Solid line: modeling based on Eq. (3) for $m = 1$.

cident angles, Eq. (3) correctly predicted the absolute angular locations of all peaks in the data. The calculation also yields reasonable agreement with the measured intensity ratio. The residual difference could be due to instrumental broadening, low material contrast, and finite travel length in the multilayer, as well as dynamical corrections.

The lateral length scale for scattering in the multilayer can be estimated as follows. In reciprocal space, lattice points representing the multilayer are separated vertically by $1/d$. In order for a horizontal wave vector to be scattered by an angle α to the $m=1$ order, the reciprocal-lattice points must have a horizontal width of at least $\sim \alpha/d$. In real space, that means the average scattering length in the multilayer is no more than $d/\alpha = 5400 \text{ \AA}$ for $\alpha \sim 2^\circ$. The scattering is caused by distortion of the wave fronts traveling in the W and the Si layers. The estimated length is reasonable considering the π -phase shift length in W and that the differential absorption between Si and W also contributes to the scattering. In a nonideal multilayer, the scattering may also be due to mosaic spread and other imperfections. The finite scattering length thus accounts for the wave-vector transfer Δk_x in the lateral direction.

The traveling-wave model discussed above adequately explains the doublet structure. An equally valid treatment is to examine independently the two components of the interference field, the incident and the reflected part. Then diffraction of the incident beam by the multilayer structure can give rise to peak A in Fig. 4, while diffraction of the totally reflected beam by the multilayer can account for peak B. The peaks' locations will be identical to those predicted from the traveling-wave model. The difference will be only in the intensity distribution, as the traveling-wave approach is correct when the superimposing waves are coherent, while the kinematic two-beam method should apply when the reflected beam is incoherent with the incident beam. Factors affecting the coherence, such as the x-ray source and the sample roughness, need to be considered. The longitudinal coherence length l_c due to the source is about $\lambda^2/8\lambda \approx 1200 \text{ \AA}$. Because of the grazing geometry, the optical path difference between the beam reflected from Pt and the incident beam at the top surface is about $(2\theta)t$, where t is the thickness of the multilayer. For our case, $t = 466 \text{ \AA}$ and therefore the optical path difference is far smaller than l_c . The traverse coherence length of the source is given by $\lambda D/2S$, where D is the source-to-sample distance and S is the source size. For $D = 1.26 \text{ m}$ and $S \approx 1 \text{ mm}$, the traverse coherence length is on the or-

der of 1000 \AA , which represents a length of $10\text{--}20 \mu\text{m}$ when projected onto the sample surface. Thus the sample was illuminated with partially coherent radiation. The coherence of the radiation can be further degraded by sample factors such as roughness and layer interdiffusion. In this situation only rigorous calculations, including all the experimental factors, can distinguish between the two models from the intensity distribution of the doublet and its side peaks; that is beyond the scope of this paper.

The existence of the doublet structure presents a real problem of which one needs to be aware when using x-ray interference techniques for the study of thin-film structures. In specular reflectivity measurements of films deposited on an optically dilute material, such as the sample used in our experiment and that used in the experiment of Ref. 6, the x-rays giving rise to the doublet structure as well as the asymmetric Bragg reflection may need to be included in the analysis of the specular reflectivity spectrum. For techniques employing asymmetric Bragg reflection, the doublet structure could complicate the data analysis due to mixing with the interference fringes arising from the asymmetric Bragg scattering.

CONCLUSION

The study of nonspecular scattering of x rays from a multilayer structure deposited on a Pt film revealed the origin of the doublet structure first observed about three decades ago. The origin of this doublet structure had remained a long-standing problem. It can be explained by diffraction of the traveling component of the interference field formed by the incident beam and the specularly reflected beam when the sample is coherently illuminated. When the sample is not coherently illuminated, the doublet can also be explained in terms of the diffraction of the incident and the reflected beams, respectively, by the multilayer. Under both illumination conditions, the angular position of the doublet structure will be the same but the intensities of the peaks will be different. The sample in our experiment was illuminated with partially coherent x rays, and thus our experimental results can be explained reasonably well by either theory.

ACKNOWLEDGMENTS

The authors would like to thank S. Durbin for pointing out the two-beam model and for other suggestions. This work was supported by the U.S. Department of Energy, BES-Materials Science, under Contract No. W-31-109-Eng-38.

¹H. Kiessig, *Ann. Phys.* **10**, 715 (1931).

²C. A. Melendres, H. You, V. A. Maroni, Z. Nagy, and W. Yun, *J. Electrical. Chem.* **297**, 549 (1991).

³D. Schwartz, A. Braslau, B. Ocko, P. S. Pershan, J. Als-Nielsen, and J. S. Haug, *Phys. Rev. A* **38**, 5817 (1988).

⁴I. M. Tidswell, B. M. Ocko, P. S. Pershan, S. R. Wasserman, G. M. Whitesides, and J. D. Axe, *Phys. Rev. B* **41**, 1111 (1990).

⁵J. Sauro, I. Fankuchen, and N. Wainfan, *Phys. Rev.* **132**, 1544 (1963).

⁶D. S. Kapp and N. Wainfan, *Phys. Rev.* **138**, A1490 (1965).

⁷W. B. Yun and J. M. Bloch, *J. Appl. Phys.* **68**, 1421 (1990).

⁸T. Ishikawa, A. Iida, and T. Matsushita, *Nucl. Instrum. Methods A* **246**, 348 (1986).

⁹R. W. James, *The Optical Principles of the Diffraction of X-Rays* (Ox Bow, Woodbridge, CT, 1982).

¹⁰M. J. Bedzyk, G. M. Bommarito, and J. S. Schildkraut, *Phys. Rev. Lett.* **62**, 1376 (1989).

¹¹See, for instance, M. J. Bedzyk, D. H. Bilderback, G. M. Bommarito, M. Caffrey, and J. S. Schildkraut, *Science* **241**, 1788

(1988); H. D. Abruna, G. M. Bommarito, and D. Acevedo, *ibid.* **250**, 69 (1990).

¹²M. Born and E. Wolf, *Principles of Optics*, 6th ed. (Pergamon, New York, 1980).